Inventory of Supplemental Information

Figure S1: Flow cytometric analysis, related to Figure 1.

Figure S2: Analysis of transplanted mice, related to Figures 2 and 3.

Figure S3: 4-week analysis of HSC subtypes using single cell transplantation, related to Figure 4.

Figure S4: Verification of expression of differentially expressed microarray genes by real-time PCR, related to Tables S2-4.

Figure S5: Cell cycle and proliferative status of HSC subtypes, related to Figure 6.

Figure S6: Effects of TGFβ1 and -3 on HSC subtypes, related to Figure 6.

Figure S7: Gating scheme for analysis of effect of TGFβ1 on transplanted My-HSC and Ly-HSC populations, related to Figure 6.

Table S1: Statistical measures for transplantation studies, related to Figures 2-5.

Table S2: Probe information for all microarray chips.

Table S3: Genes upregulated in My-HSCs compared to Ly-HSCs.

Table S4: Genes upregulated in Ly-HSCs compared to My-HSCs.

Distinct Hematopoietic Stem Cell Subtypes Are Differentially Regulated by TGFβ1

Grant A. Challen, Nathan C. Boles, Stuart M. Chambers and Margaret A. Goodell

SUPPLEMENTAL FIGURES:

A

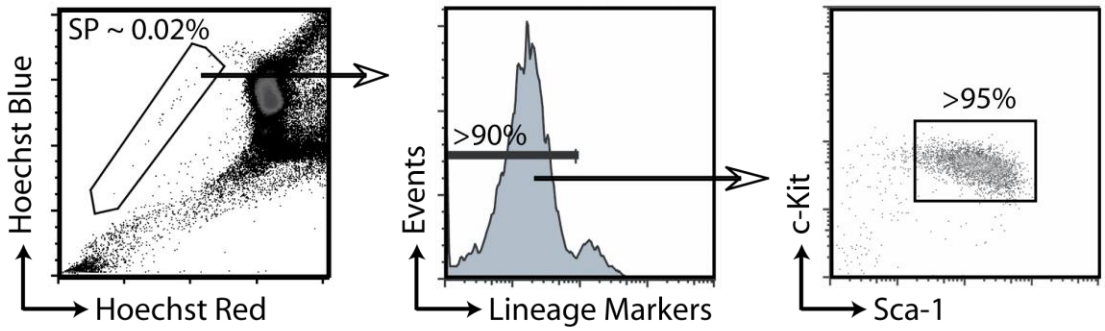

B

	MFI of Indicated Marker	
Marker	Lower-SP	Upper-SP
Sca-1	425.5	373.6
c-Kit	175.6	185.2
EPCR	68.8	61.1
CD34	140.5	172.3
Flk-2	13.1	16.3
CD150	193.2	51.4

Figure S1: Flow cytometric analysis.

(A) Side population^{+} Lineage^{-} Sca-1^{+} c-Kit^{+} (SP^{KLS}) gating strategy used for HSC purification. (B) Comparison of expression of common HSC markers on lower- and upper-SP^{KLS} cells by mean fluorescent intensity.

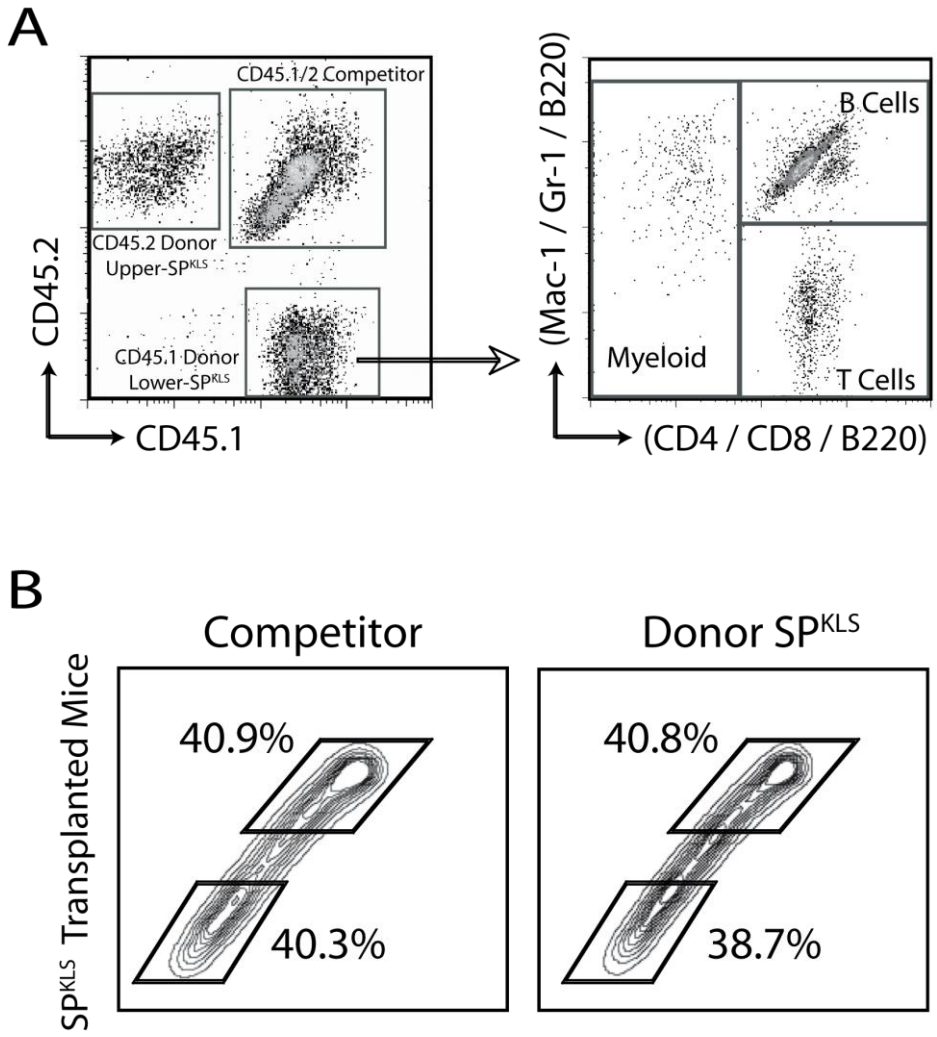

Figure S2: Analysis of transplanted mice.

(A) Peripheral blood sample of a mouse co-transplanted with lower- ($CD45.1^+$) and upper-SP^{KLS} cells ($CD45.2^+$) and competitor whole bone marrow ($CD45.1/2^+$) showing clear distinction of the progeny of each transplanted population in the peripheral blood. The lower-SP^{KLS}-derived population is then gated for lineage distribution analysis showing myeloid, B-cell and T-cell populations. (B) Analysis of the bone marrow of mice transplanted with unfractionated SP^{KLS} along with whole bone marrow competitor for SP distribution of donor cells. In reference to the whole bone marrow competitor cells which serve as an internal control, transplantation of unfractionated SP^{KLS} donor cells regenerates the entire SP in an unbiased manner. Data presented are representative of two separate experiments.

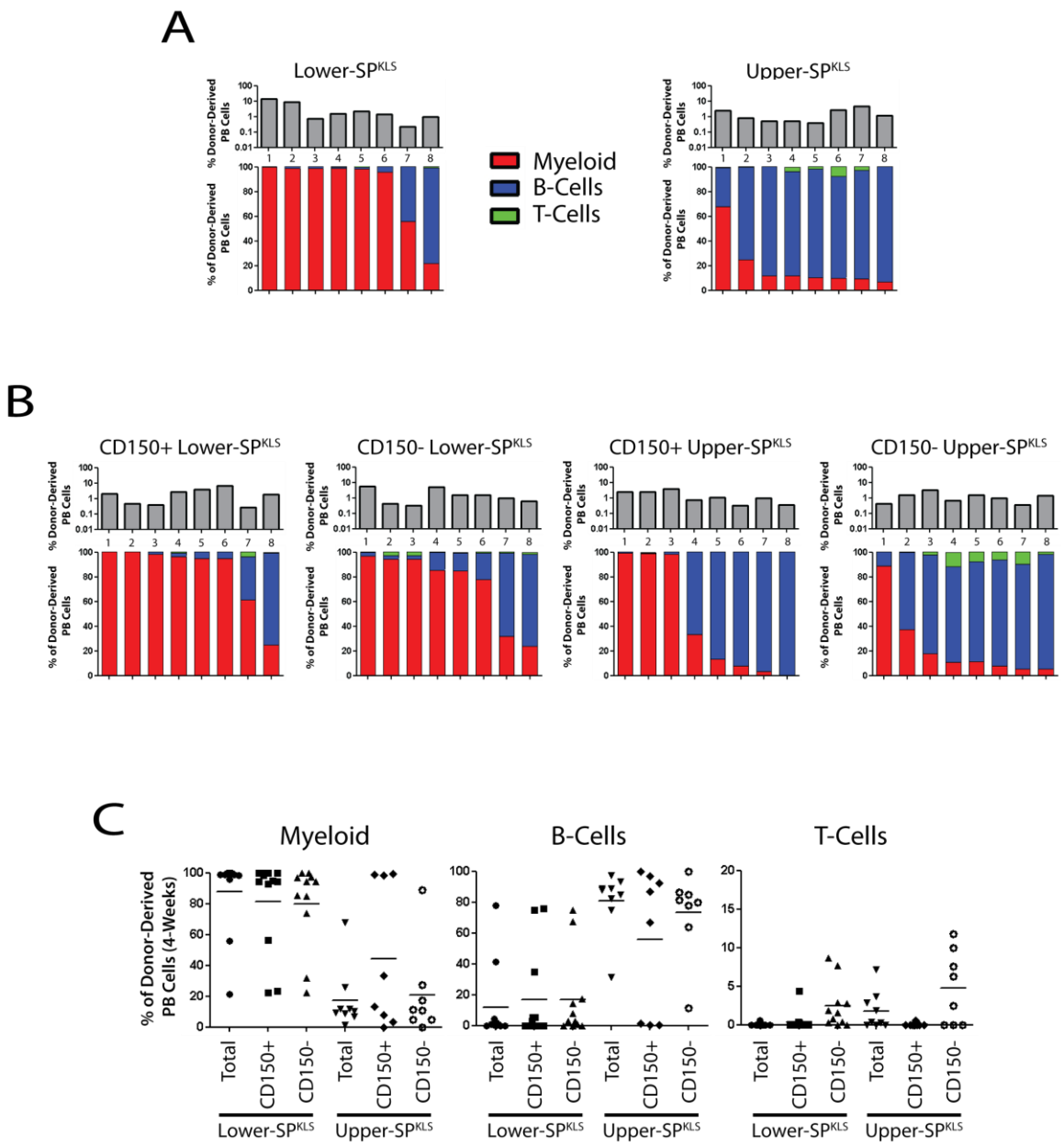

Figure S3: 4-week analysis of HSC subtypes using single cell transplantation.

(A) Tracking of eight individual lower- and upper-SP^{KLS} clones showing overall hematopoietic chimerism in recipient mice (engraftment) and lineage distribution of test cells 4-weeks post-transplant. (B) Further fractionation of these populations using the CD150 marker showed subtle differences. (C) Cumulative 4-week lineage output data from a large cohort of mice transplanted with single HSCs.

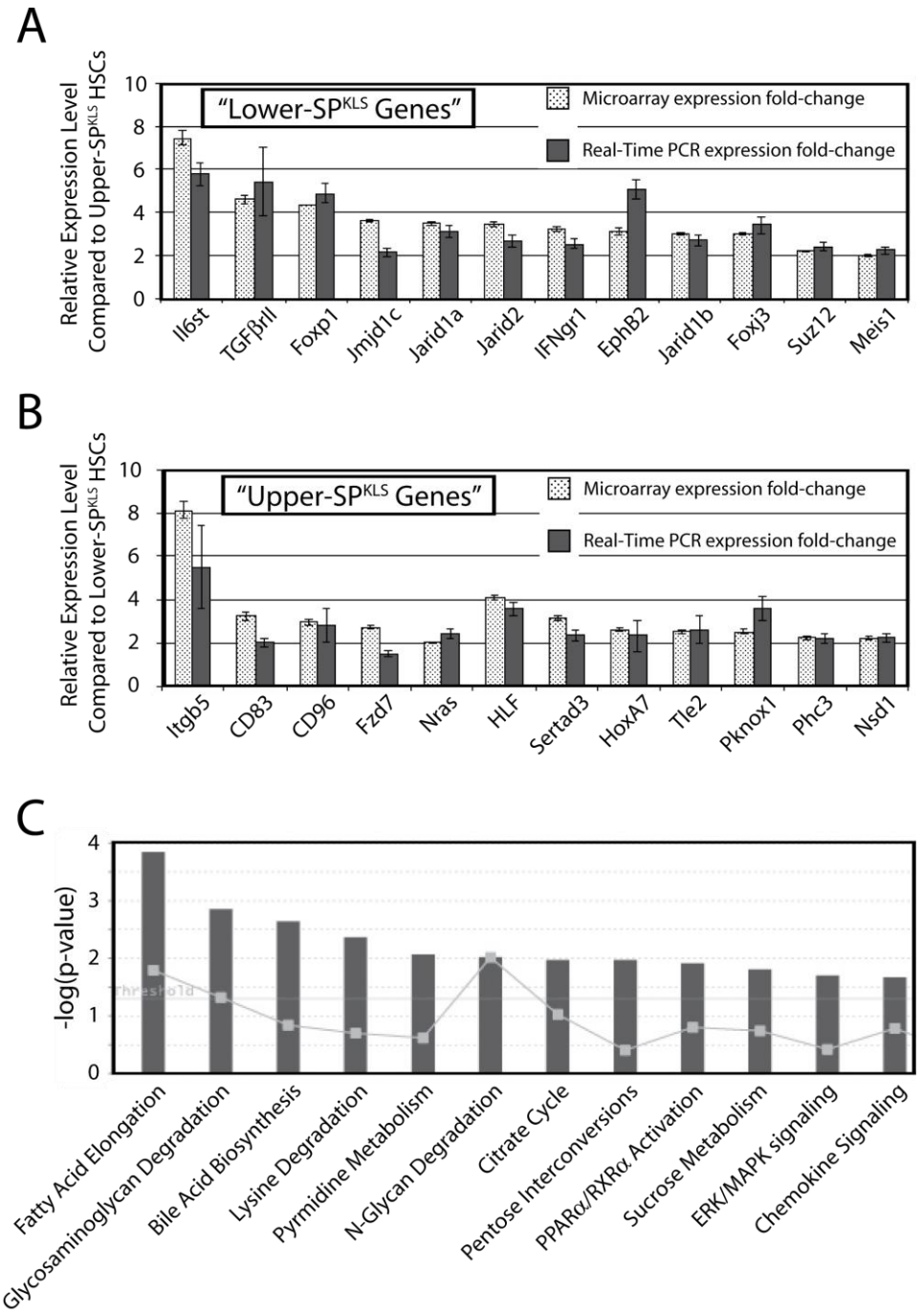

Figure S4: Verification of expression of differentially expressed microarray genes by real-time PCR.

Genes identified in microarrays as upregulated in lower-SP^{KLS} cells (A) and upper-SP^{KLS} cells (B) showed similar expression profiles when assessed by real-time PCR. (C) Ingenuity Pathway Analysis of microarray data revealed that 9 of the 12 significantly upregulated molecular pathways in upper-SP^{KLS} cells were associated with metabolism and cell cycle, reflecting the more active nature of these HSCs.

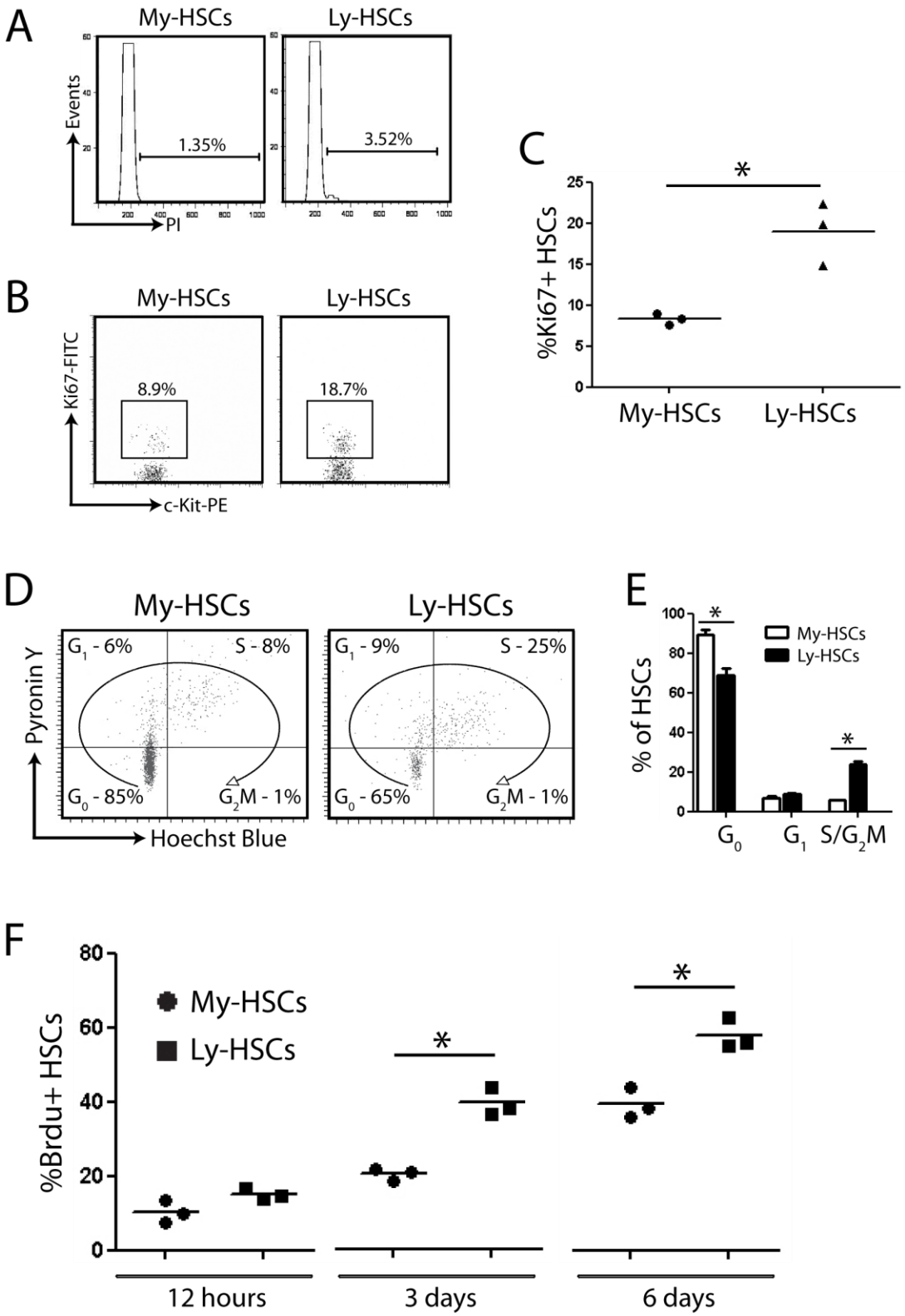
A
My-HSCs
Ly-HSCs
Events
1.35%
3.52%
PI
B
My-HSCs
Ly-HSCs
Ki67-FITC
8.9%
18.7%
c-Kit-PE
C
%Ki67+ HSCs
My-HSCs
Ly-HSCs
D
My-HSCs
Ly-HSCs
Pyronin Y
G1 - 6%
S - 8%
G0 - 85%
G2M - 1%
G1 - 9%
S - 25%
G0 - 65%
G2M - 1%
Hoechst Blue
E
% of HSCs
My-HSCs
Ly-HSCs
G0
G1
S/G2M
F
%Brdu+ HSCs
My-HSCs
Ly-HSCs
12 hours
3 days
6 days

Figure S5: Cell cycle and proliferative status of HSC subtypes.

(A) Cell cycle analysis of purified My-HSC and Ly-HSC populations using propidium iodide staining showed on average that approximately 1% and 3% respectively of these HSC subtypes were in cycle at any given point in time under homeostatic conditions. Data presented are averages of three separate experiments. (B) Example of flow cytometric analysis of My- and Ly-HSCs for Ki67 expression. (C) Comparing three separate pools of three mice, Ly-HSCs cells showed significantly higher expression of the Ki67 protein, indicating they are more active in the cell cycle at any given point in time compared to My-HSCs. (D) Example of cell cycle status analysis of My- and Ly-HSCs by Pyronin Y staining. (E) My-HSCs consistently contained a higher proportion of HSCs in G_0, or quiescence (three separate pools of three mice). (F) BrdU labeling showed that over three time periods tested (12-hours, 3-days, 6-days), the Ly-HSC population contained a higher proportion of $BrdU^+$ cells compared to My-HSCs, indicating more of this HSC subtype had turned over during these time frames (three separate pools of three mice).

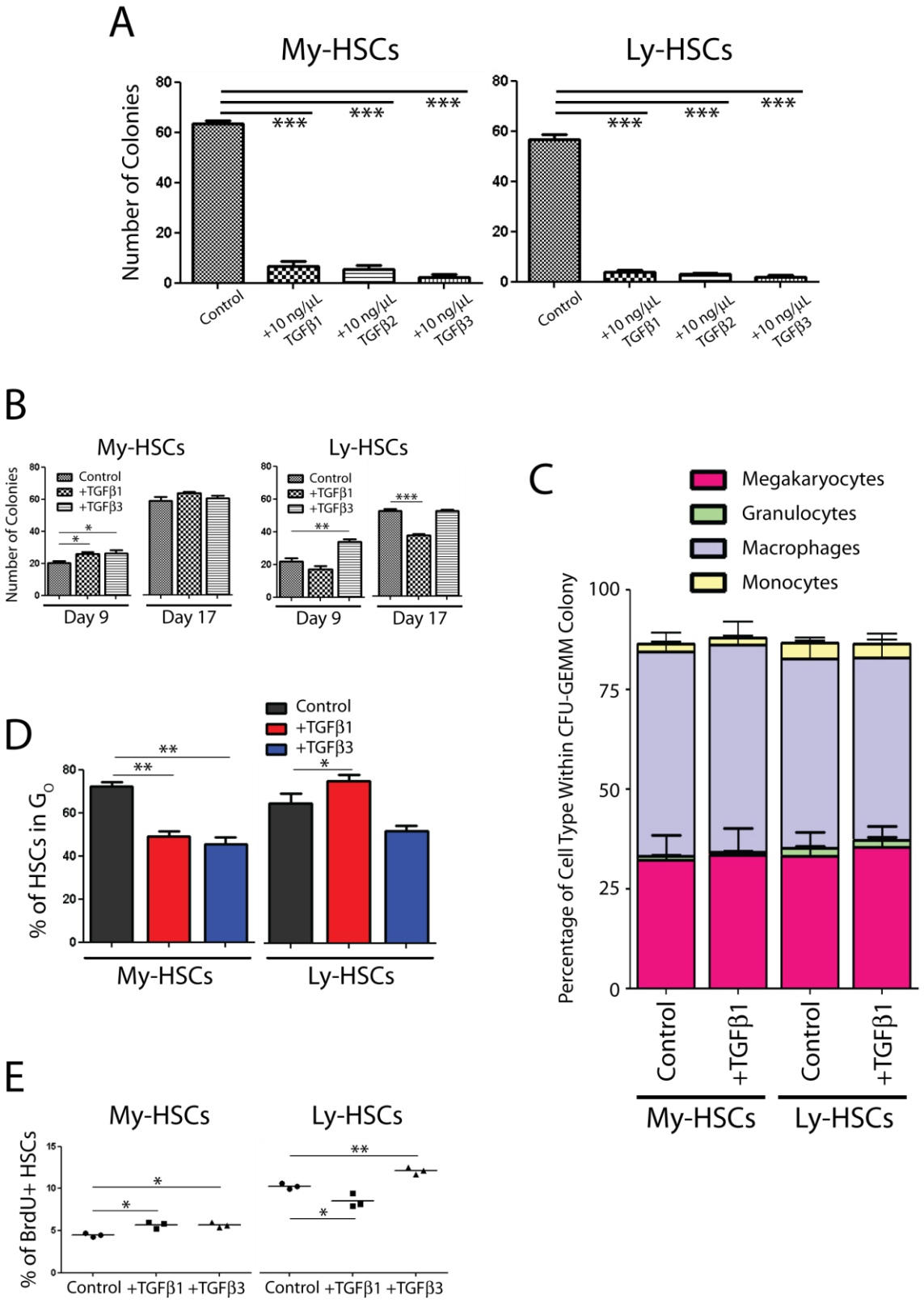
A
My-HSCs
Ly-HSCs
Number of Colonies
Control
+10 ng/µL TGFβ1
+10 ng/µL TGFβ2
+10 ng/µL TGFβ3
***
B
My-HSCs
Ly-HSCs
Control
+TGFβ1
+TGFβ3
Number of Colonies
Day 9
Day 17
C
Megakaryocytes
Granulocytes
Macrophages
Monocytes
Percentage of Cell Type Within CFU-GEMM Colony
Control
+TGFβ1
My-HSCs
Ly-HSCs
D
% of HSCs in G0
E
% of BrdU+ HSCs

Figure S6: Effects of TGFβ1 and -3 on HSC subtypes. (TGFβ2 produced the same responses in My-HSCs and Ly-HSCs as TGFβ1).

(A) Single My-HSCs (lower-SP^{KLS}) or Ly-HSCs (upper-SP^{KLS}) were sorted into individual wells of 96-well plates containing Methocult + 10 ng/μL TGFβ's. At this concentration, all TGFβ's strongly inhibited colony formation from both My- and Ly-HSCs. Data presented are cumulative of three individual experiments each comprising two replicate plates for each condition. (B) Low (10 pg/μL) concentrations of TGFβ's accelerated colony formation of My-HSCs in Methocult (more colonies at day 9), but did not change the total number of colonies formed (at day 17). While TGFβ1 proved inhibitory to Ly-HSC colony formation, addition of TGFβ3 was stimulatory as for My-HSCs. Data presented are cumulative of three individual experiments each comprising two replicate plates for each condition. (C) TGFβ1 did not change the distribution of myeloid cell types within individual CFU-GEMM colonies. Flow cytometric analysis of CFU-GEMM colonies with the proportion of cell types represented comprised of megakaryocytes ($CD41^+$), granulocytes ($Mac\text{-}1^+Gr\text{-}1^+F4/80^-$), macrophages ($Mac\text{-}1^+F4/80^+$) and monocytes ($Mac\text{-}1^+Gr\text{-}1^-F4/80^-$). Data presented are averages of two individual experiments each comprising analysis of 20 individual CFU-GEMM colonies. (D) Pyronin Y staining of My- and Ly-HSCs following 5-hour *in vitro* exposure to TGFβ's. All TGFβ's stimulated My-HSCs to engage the cell cycle with a lower portion of this population in G_0 compared to control cells following TGFβ exposure. Conversely, exposure to TGFβ1 impeded the normal progression into cell cycle of Ly-HSCs with a higher proportion of this population in G_0 following *in vitro* culture. Data presented are averages of four individual experiments. (E) Effect on HSC subtypes to *in vivo* TGFβ exposure. Injection of mice with 0.1 μg TGFβ's caused an increase in proliferation of My-HSCs. *in vivo* administration of TGFβ1 inhibited Ly-HSC proliferation while TGFβ3 enhanced the proliferation of this HSC subtype (three separate pools of three mice).

.

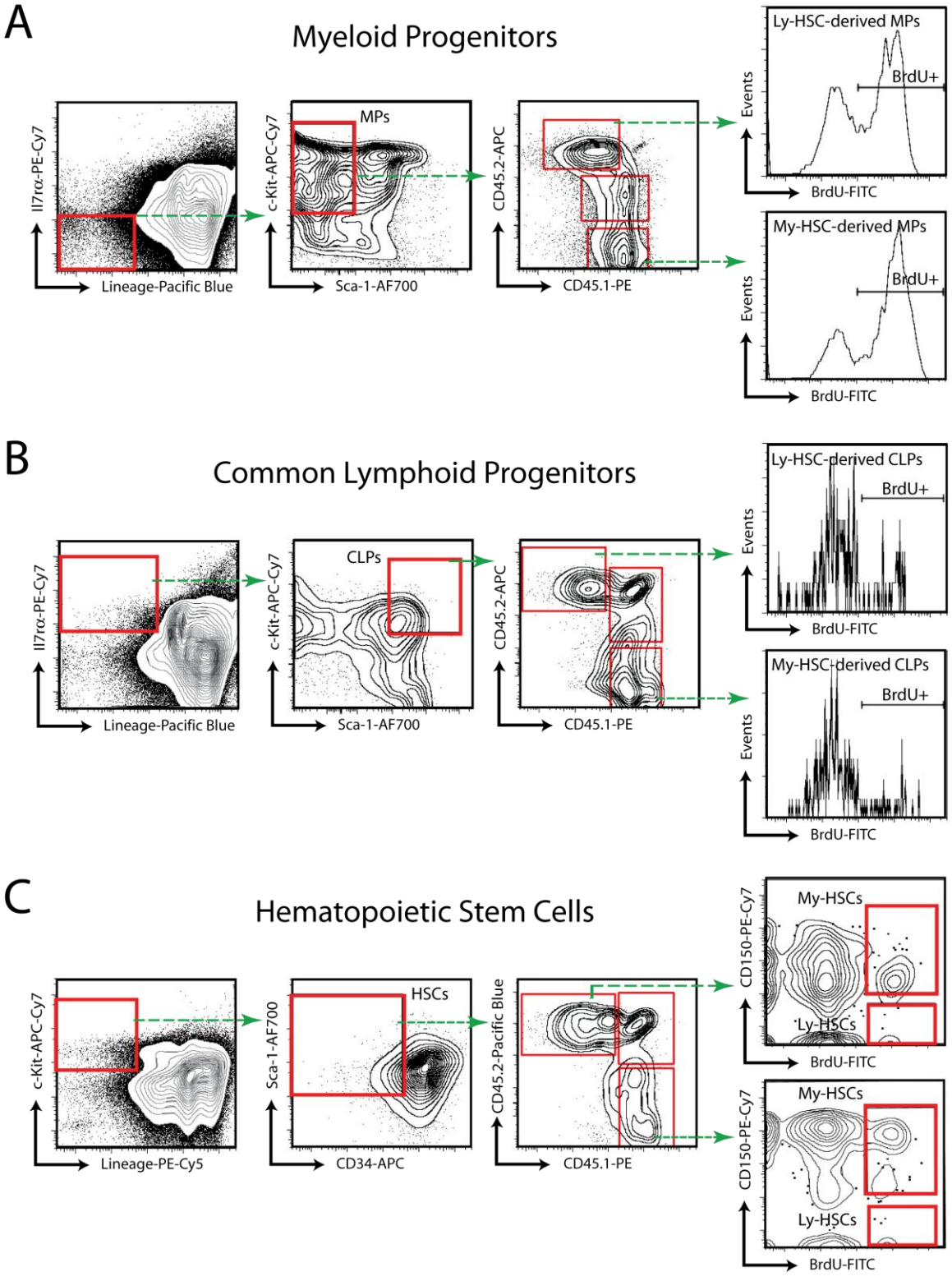
A
Myeloid Progenitors
IL7rα-PE-Cy7
Lineage-Pacific Blue
c-Kit-APC-Cy7
MPs
Sca-1-AF700
CD45.2-APC
CD45.1-PE
Ly-HSC-derived MPs
BrdU+
Events
BrdU-FITC
My-HSC-derived MPs
BrdU+
Events
BrdU-FITC
B
Common Lymphoid Progenitors
IL7rα-PE-Cy7
Lineage-Pacific Blue
c-Kit-APC-Cy7
CLPs
Sca-1-AF700
CD45.2-APC
CD45.1-PE
Ly-HSC-derived CLPs
BrdU+
Events
BrdU-FITC
My-HSC-derived CLPs
BrdU+
Events
BrdU-FITC
C
Hematopoietic Stem Cells
c-Kit-APC-Cy7
Lineage-PE-Cy5
Sca-1-AF700
HSCs
CD34-APC
CD45.2-Pacific Blue
CD45.1-PE
CD150-PE-Cy7
My-HSCs
Ly-HSCs
BrdU-FITC
CD150-PE-Cy7
My-HSCs
Ly-HSCs
BrdU-FITC

Figure S7: Gating scheme for analysis of effect of TGFβ1 on transplanted My-HSC and Ly-HSC populations.

Lethally irradiated CD45.1/2 mice were transplanted with 25 CD45.1 lower-SP^{KLS} My-HSCs and 50 CD45.2 upper-SP^{KLS} Ly-HSCs (along with 200,000 CD45.1/2 whole bone marrow competitor cells). 12-weeks post-transplant, test mice were administered three 0.1 μg TGFβ1 injections 24-hours apart and then labeled with BrdU 12-hours prior to sacrifice to determine the effect of TGFβ1 on turnover rate of various donor cell-derived stem and progenitor cell compartments. Stem and progenitor cells were identified using the following phenotypes (A) myeloid progenitors – $Lineage^{-}Il7r\alpha7^{-}Sca\text{-}1^{-/low}c\text{-}Kit^{+}$ (B) common lymphoid progenitors - $Lineage^{-}Il7r\alpha7^{+}Sca\text{-}1^{+}c\text{-}Kit^{+}$ (C) myeloid-biased HSCs - $Lineage^{-}c\text{-}Kit^{+}Sca\text{-}1^{+}CD34^{-}CD150^{+}$ and lymphoid-biased HSCs $Lineage^{-}c\text{-}Kit^{+}Sca\text{-}1^{+}CD34^{-}CD150^{-}$. Transplanted donor My-HSCs ($CD45.1^{+}$) and Ly-HSCs ($CD45.2^{+}$) were distinguished from competitor marrow ($CD45.1^{+}CD45.2^{+}$) using a combination of CD45 alleles and the turnover of each donor-derived cell compartment in response to TGFβ1 was assessed by comparing the percentage of $BrdU^{+}$ cells relative to control transplanted mice (PBS-injected).

SUPPLEMENTAL TABLES:

Table S1: Statistical measures for transplantation studies.

Table S2: Probe information for all microarray chips.

Table S3: Genes upregulated in My-HSCs compared to Ly-HSCs.

Table S4: Genes upregulated in Ly-HSCs compared to My-HSCs.

SUPPLEMENTAL EXPERIMENTAL PROCEDURES:

HSC Cell Cycle Analysis

1) Propidium iodide staining: HSCs (>1500) were sorted into deionized water containing 0.1% sodium citrate and 50μg/mL propidium iodide (PI) and analyzed with a FACScan flow cytometer (BD Biosciences).

2) BrdU Incorporation Analysis: Mice received one intraperitoneal injection of BrdU (Sigma-Aldrich; 1 mg/6 g of mouse weight), followed by inclusion of BrdU in the drinking water at 0.8 mg/mL. Mice were sacrificed at 12-hours, three days and six days post-BrdU injection and HSCs were sorted from Sca-1 enriched bone marrow as (lower- or upper-) SP^+ Lineage-PE-$Cy5^-$ c-Kit-PE^+ cells into a carrier cell population of 400,000 B220-PE-$Cy5^+$ splenocytes. Samples were prepared for analysis of BrdU incorporation using the FITC-BrdU Flow Kit (BD Pharmingen). Samples were reanalyzed by flow cytometry with HSCs readily distinguishable from B220-PE-$Cy5^+$ carrier cells as c-Kit-PE^+ B220-PE-$Cy5^-$ and were gated for analysis of BrdU-FITC incorporation.

3) Ki67 Analysis: HSCs were sorted from pools of mice as described above into a carrier cell population of 400,000 B220-PE-$Cy5^+$ splenocytes. Sorted samples were prepared using the FITC-BrdU Flow Kit (BD Pharmingen) with the substitution of anti-Ki67-FITC (BD Pharmingen) for anti-BrdU-FITC. Samples were reanalyzed by flow cytometry and HSCs were gated for analysis of Ki67-FITC incorporation.

Table: Details of antibodies used for flow cytometry.

Epitope	Clone	Conjugate	Dilution	Company
Gr-1	RB6-8C5	PE-Cy5	1:100	eBioscience
	RB6-8C5	FITC	1:100	BD Pharmingen
	RB6-8C5	Biotin	1:100	BD Pharmingen
	RB6-8C5	PE-Cy7	1:100	eBioscience
Mac-1	M1/70	PE-Cy5	1:100	eBioscience
	M1/70	FITC	1:100	BD Pharmingen
	M1/70	Biotin	1:100	BD Pharmingen
	M1/70	PE-Cy7	1:100	BD Pharmingen
B220	RA3-6B2	PE-Cy5	1:100	eBioscience
	RA3-6B2	FITC	1:100	BD Pharmingen
	RA3-6B2	Biotin	1:100	BD Pharmingen
	RA3-6B2	PE-Cy7	1:100	BD Pharmingen
	RA3-6B2	Pacific Blue	1:100	BD Pharmingen
Ter119	TER119	PE-Cy5	1:100	eBioscience
	TER119	FITC	1:100	BD Pharmingen
	TER119	Biotin	1:100	BD Pharmingen
CD4	RM4-5	PE-Cy5	1:100	eBioscience
	GK1.5	FITC	1:100	BD Pharmingen
	H129.19	Biotin	1:100	BD Pharmingen
	RM4-5	Pacific Blue	1:100	BD Pharmingen
CD8	53-6.7	PE-Cy5	1:100	eBioscience
	53-6.7	FITC	1:100	BD Pharmingen
	53-6.7	Biotin	1:100	BD Pharmingen
	53-6.7	Pacific Blue	1:100	BD Pharmingen
CD3	145-2C11	Biotin	1:100	BD Pharmingen
CD19	1D3	Biotin	1:100	BD Pharmingen
Sca-1	E13-161.7	PE	1:100	BD Pharmingen
	E13-161.7	FITC	1:100	BD Pharmingen
	D7	APC	1:100	eBioscience
	D7	PE-Cy7	1:100	eBioscience
	E13-161.7	Biotin	1:100	BD Pharmingen
c-Kit	2B8	PE	1:100	BD Pharmingen
	2B8	FITC	1:100	BD Pharmingen
	2B8	APC	1:100	eBioscience
	2B8	AlexaFluor-750	1:100	eBioscience
	2B8	Biotin	1:100	eBioscience
Il7rα	A7R34	PE-Cy7	1:100	eBioscience
Flk-2	A2F10.1	PE	1:50	BD Pharmingen
CD34	RAM34	AlexaFluor-647	1:50	eBioscience
CD150	TC15-12F12.2	PE	1:100	BioLegend
	TC15-12F12.2	PE-Cy7	1:100	BioLegend
EPCR	RMEPCR1560	FITC	1:100	StemCell Technologies
CD45.1	A20	PE	1:100	BD Pharmingen
	A20	FITC	1:100	BD Pharmingen
	A20	Biotin	1:100	BD Pharmingen
CD45.2	104	PE	1:100	eBioscience
	104	APC	1:100	eBioscience
	104	Biotin	1:100	eBioscience
CD48	HM48-1	APC	1:100	eBioscience